CONFIGURATION OF STIFFENED PANELS

The configuration of the panels is shown in figure 1. They were 12 inches wide and 24 inches long between the grips of the testing machine. The sheet and stringers were made with graphite/epoxy prepreg tape. The graphite fibers were T300 made by Union Carbide and the epoxy was 5208 made by Narmco Materials Inc. The sheet and stringers were cocured with film adhesive added to the stringer-sheet interface. The sheets were 16 plies thick and made with $(45/0/-45/90)_{2s}$ and $(45/0/-45/0)_{2s}$ layups. The stringers were unidirectional and had various widths and thicknesses. The values of stringer area were chosen such that the ratios of stringer stiffness to panel stiffness μ were 0.3, 0.5, and 0.7. Consequently, for a given stiffness ratio, the stringers were thicker for the stiffer $(45/0/-45/0)_{2s}$ sheets than for the $(45/0/-45/90)_{2s}$ sheets.

Three or six panels were made of each type. The panels were loaded in tension at the ends to produce uniform axial strain parallel to the stringers. Load and not displacement was controlled. Crack-like slots of various lengths were machined into the sheets at the middle of the panels to represent damage.

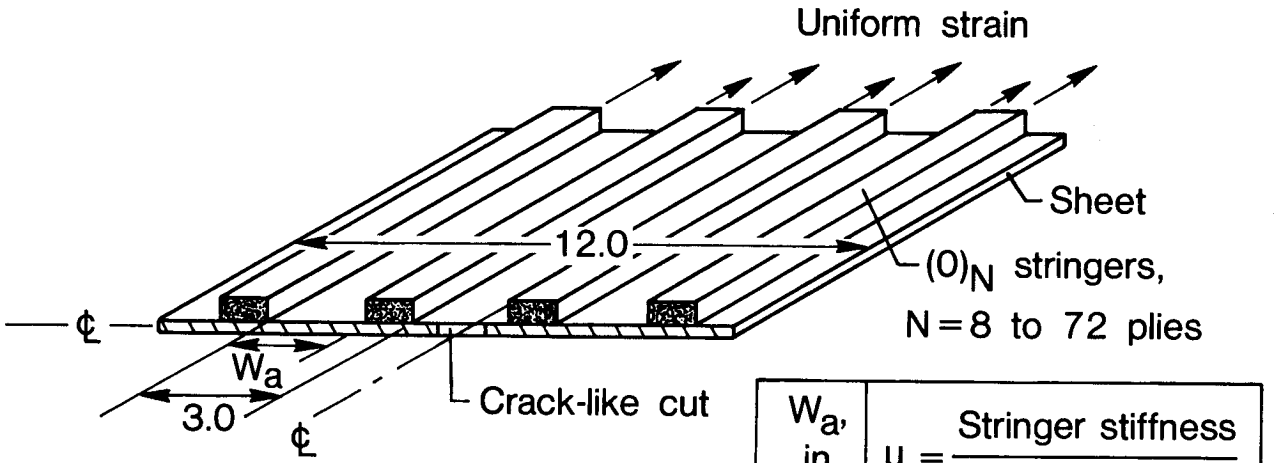

W_a, in.	$\mu = \frac{\text{Stringer stiffness}}{\text{Panel stiffness}}$
2.0	0.3
.5 2.0 2.5	.5
2.0	.7

Figure 1

TEST RESULTS FOR $(45/0/-45/90)_{2S}$ PANELS WITH $\mu = 0.7$

First, some typical test results are presented to show how the cracks initiated and were arrested. Strain versus crack tip position is shown in figure 2 for the three $(45/0/-45/90)_{2S}$ with $\mu = 0.7$. As the panels were loaded, cracks initiated and ran from the slot ends at strains that correspond to the the failing strains of unstiffened sheets. (The failing-strain curve without stringers is associated with initial crack length or slot length, not final length. Thus, the strains at instability actually agree better with the curve than indicated.) For the shortest slot, the crack was not arrested. But for the longest slots, the stringers arrested the cracks and loading was continued. Eventually, the sheet and stringers appeared to fail simultaneously at a strain considerably larger than that for a sheet without stringers. This behavior is typical of all the panels. Usually, when cracks were not arrested, failing strains were greater than or equal to those when cracks were arrested.

During each test, crack-opening displacements were measured continuously, and loading was halted numerous times to make radiographs of the crack tips. An opaque dye (zinc iodide) was used to enhance the visibility of matrix damage. The radiographs and crack-opening displacements were used to estimate the crack tip positions plotted in figure 2. The last radiograph of panel C, which was made at a strain corresponding to 97 percent of the failing strain, is also shown in figure 2. (The last radiograph of panel B has the same appearance as that of panel C.) The two dark rectangular regions are the stringers. (Strain gages and wires can also be seen.) The even darker regions at the ends of the crack are disbonds between the sheet and stringers. Probably large shear stresses were the principal cause of the disbonds. The radiograph indicates that the arrested crack ran under the stringers about 1/3 inch. Usually the cracks extended to the disbond fronts.

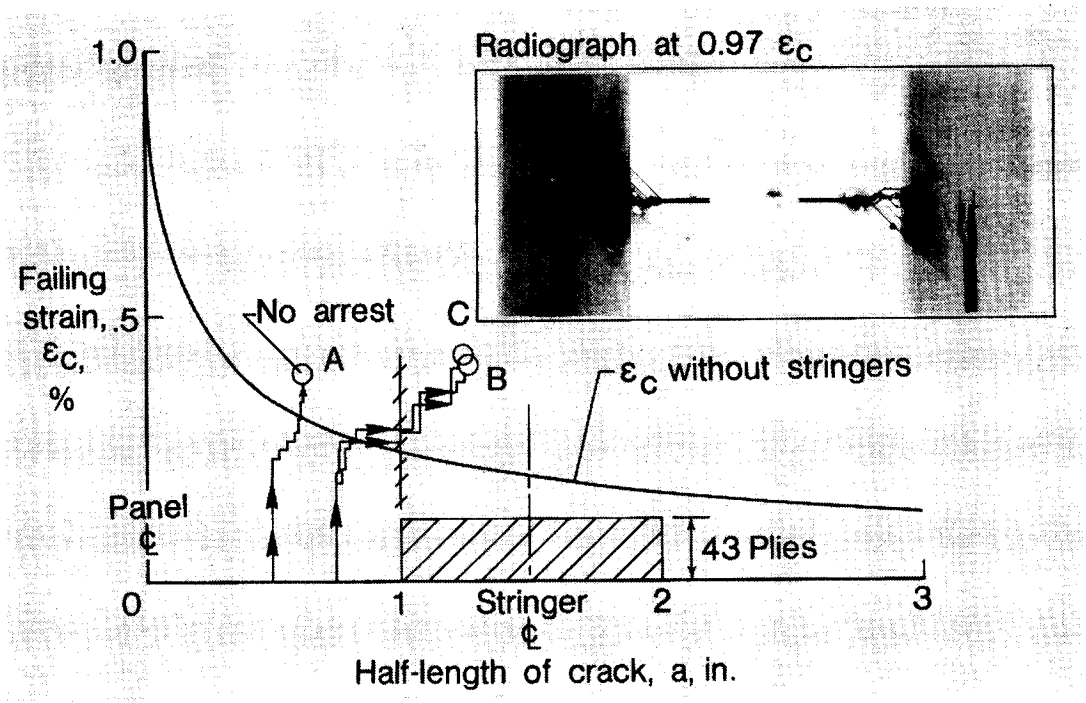

Figure 2

TEST RESULTS FOR $(45/0/-45/90)_{2S}$ PANELS WITH $\mu = 0.5$

Strain versus crack-tip position is shown in figure 3 for three of the panels with $\mu = 0.5$ and stringers of different thicknesses and widths. The initiation and arrest of cracks are similar to those in figure 2. The last radiographs are also shown in figure 3. They were made within 5 to 10 percent of the failing load. For lack of space, only one crack tip is shown. (Both crack tips had virtually the same position and appearance.) For the thinnest stringers, panel A, the crack arrested at the inside edge of the stringer. However, for the thicker stringers, panels B and C, the stringers disbonded locally, and the cracks ran beneath the stringers. For the thickest stringers, panel C, the crack ran slightly beyond the outside edge of the stringer. The shear stresses that caused the disbonds are larger for thicker stringers. Thus, although the size of disbonds varied quite a bit, they tended to be larger for thicker stringers. The variations seemed somewhat random, as though they were caused by variations in interface strength.

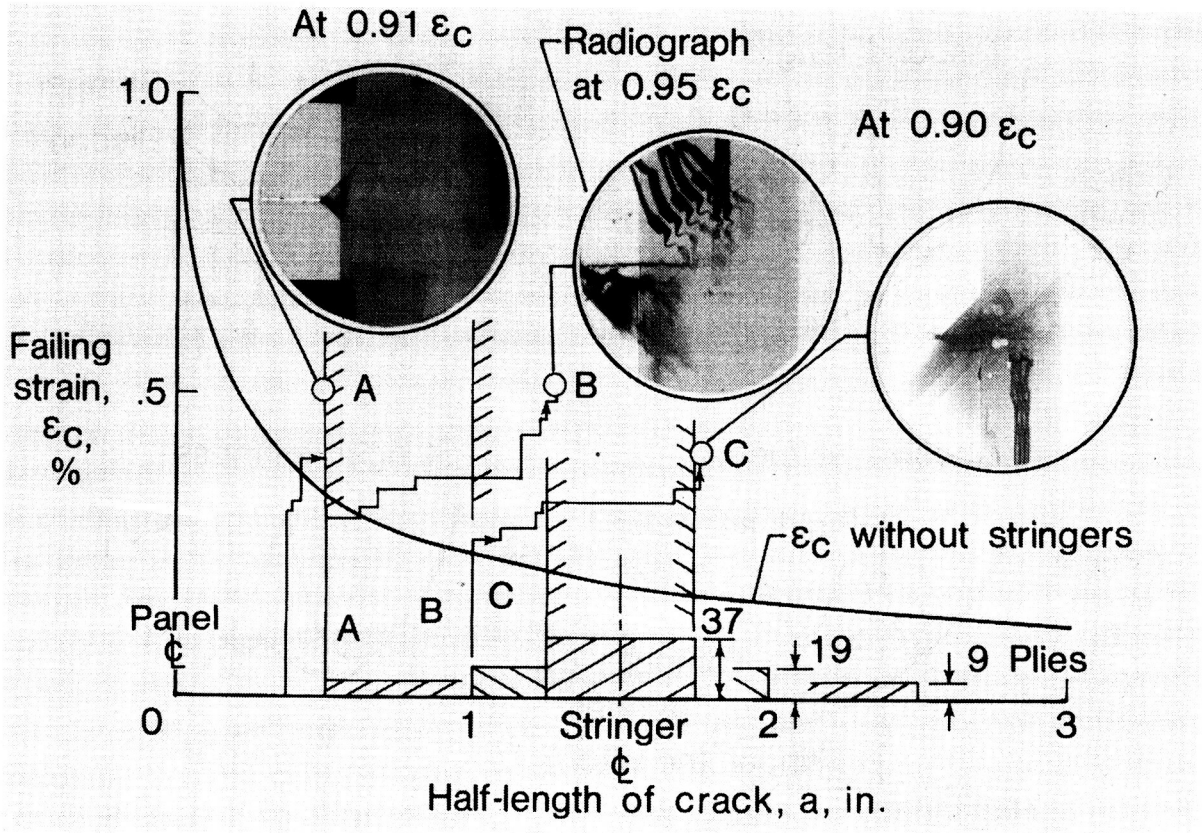

Figure 3

ANALYSIS FOR BONDED STRINGERS

The stress intensity factor has been determined for a cracked sheet with bonded and partially disbonded stringers (ref. 1). The stiffnesses of the stringers and adhesive were taken into account. The stringer was assumed to act along its centerline, that is, to have no width. For a critical value of the stress-intensity factor, the corresponding strain was calculated and plotted against half-length of crack in figure 4. Results are shown with and without stringers for different values of stringer and adhesive stiffness and disbond length. Because the stringers reduce the stress intensity factor, the critical-strain curves with stringers are above that without stringers. They have high peaks when the crack tip is just beyond the stringer. The curve is lower with a disbond ($\ell > 0$). If the stringers were completely disbonded, the curves with and without stringers would be the same. The curve is higher for a stiffer adhesive and stiffer stringers. For a rigid adhesive and $\ell = 0$, the critical strain would go to infinity for the crack tip at the stringer centerline, regardless of the stringer stiffness.

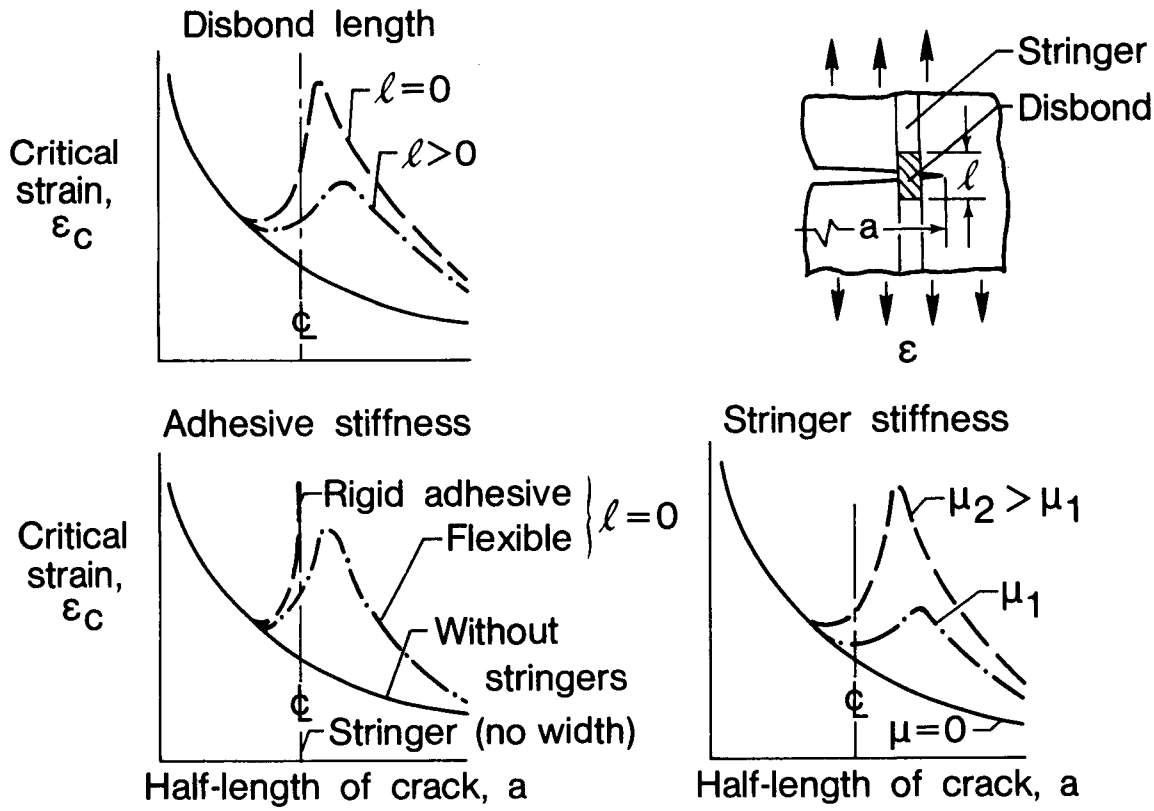

Figure 4

PREDICTING FAILING STRAINS

The critical strain is replotted against half-length of crack for different disbond lengths in figure 5. For an initial crack length of $2a_o$, the results indicate that the crack would run at a far-field strain of ε_{ci} and be arrested at the stringer if $\varepsilon_{ci} < \varepsilon_{cu}$. (Dynamic effects may require ε_{ci} to be even less for arrest.) Upon increasing the load further, the arrested crack would run at ε_{cu}. Short cracks, where $\varepsilon_{ci} > \varepsilon_{cu}$, would not be arrested, and failing strains would be greater than ε_{cu}. Thus, for arrested cracks, the failing strain ε_{cu} would be given by the peak value of ε_c, which decreases with disbond length and increases with adhesive and stringer stiffness. Also, for a given adhesive and stringer stiffness and disbond length, ε_{cu} is independent of a_o. For short cracks that are not arrested, $\varepsilon_{cu} = \varepsilon_{ci}$. Typically, the data followed this trend.

Note that thin well-bonded stringers would also have large local stresses when the crack tip approached. Thus, they could fail and reduce the failing strain below that given by the curves in figure 5.

Although this analysis gives insight into how the failing strains of stiffened panels are affected by configuration and material, it could give very inaccurate predictions. Failing strains would be greatly overestimated for wide stringers when there is little or no disbonding because the stringers are assumed to act (or to be concentrated) at their centerlines. Predictions would be more accurate if the disbond was long compared to stringer width. However, only a few panels with very thick, narrow stringers had long disbonds.

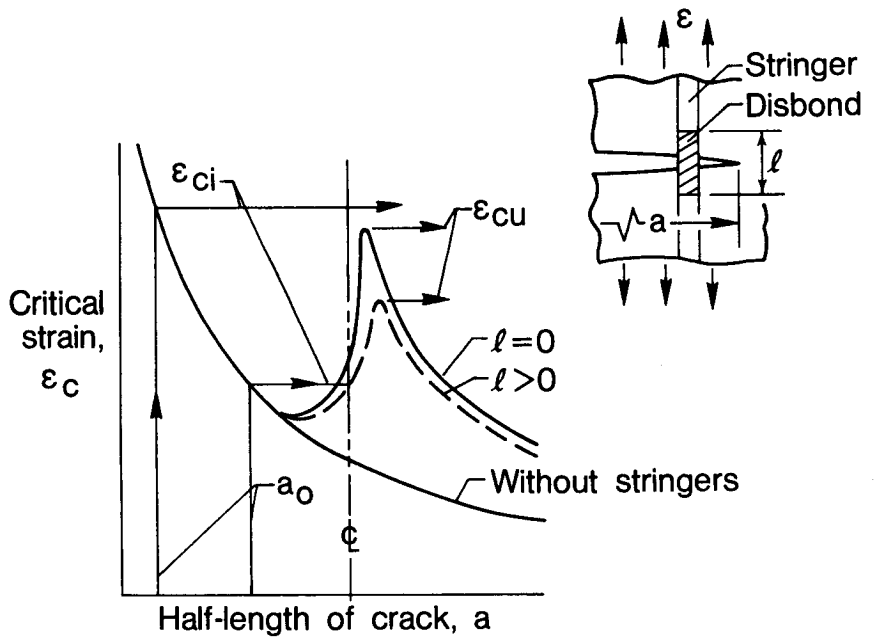

Figure 5

SHEAR LAG ANALYSIS

A shear lag analysis was made of a stiffened panel, treating the stringers and sheet as monolithic regions in the sheet. The sheet and stringers have Young's moduli E_{sh} and E_{st} in the loading direction and thicknesses t_{sh} and t_{st}, respectively. (See figure 6.) Within the region of the stringers, the stringers and sheet are assumed to act in parallel, and the stiffness is given by $(Et)_1 = (Et)_{sh} + (Et)_{st}$. The crack was assumed to extend completely across the sheet between stringers as though it were arrested.

Typical results are shown in figure 6. The logarithm of the strain concentration factor (SCF) is plotted against the logarithm of an effective crack length $W_a(Et)_{sh}/(Et)_1$ or $W_a/(1 + \alpha)$, where $\alpha = (Et)_{st}/(Et)_{sh}$. The SCF is the ratio of the strain at the crack tip to the far-field strain. (The crack tip strain is finite in the shear lag analysis.) Also, the analysis indicates that stringer width W_{st} has little effect on the SCF as long as W_{st} is large compared to a characteristic dimension of the order of fiber spacing. For $W_a = 0$, SCF = 1 as required. For a large effective crack length, SCF $\propto \sqrt{[W_a/(1 + \alpha)]}$, much as the stress intensity factor is proportional to $\sqrt{W_a}$ for an unstiffened sheet. Thus, the shear lag and stress intensity factor analyses give similar results for an unstiffened sheet $\alpha = 0$. This similarity suggests that a stress intensity factor can be synthesized using the shear lag results.

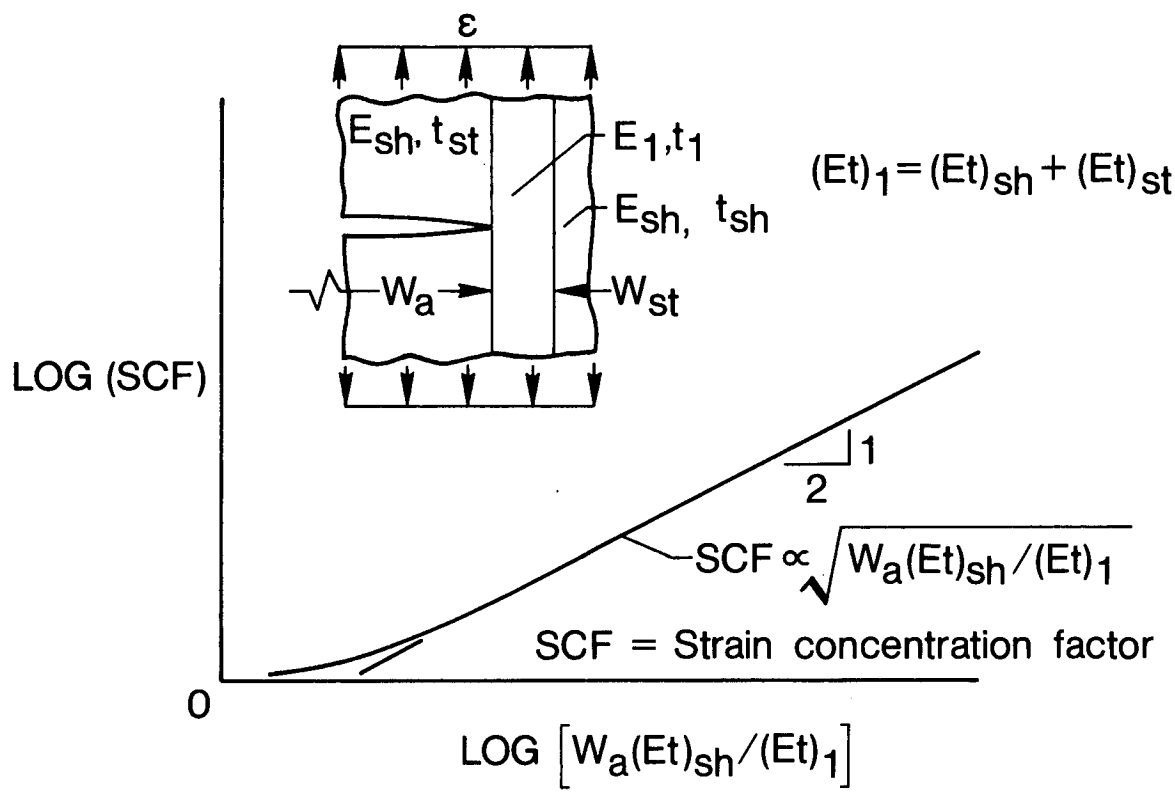

Figure 6

SYNTHESIZED STRESS INTENSITY FACTOR

Without stringers, the stress intensity factor K_Q is given by equation (1) in figure 7, where S_{sh} is the stress applied to the sheet and F_{tu} is the uncracked strength of the sheet. (Note that the stress applied to the stringer region in figure 6 is $S_{sh}E_1/E_{sh}$.) The term $(K_Q/F_{tu})^2$ was included in equation (1) to give $S_{sh} = F_{tu}$ when $a = 0$ as required. For a state of uniaxial stress, $S_{sh} = E_{sh}\varepsilon_c$ and $F_{tu} = E_{sh}\varepsilon_{tu}$. Substituting these expressions into equation (1) for stresses and solving for $\varepsilon_{tu}/\varepsilon_c$ gives equation (2) in figure 7. The left-hand side of equation (2) is equivalent to the SCF in figure 6. Replacing a in equation (2) by $\frac{1}{2} W_a/(1 + \alpha)$, the effective crack length from the shear lag results, gives equation (3) in figure 7. For small and large effective crack lengths, equation (3) models the essential features of the shear lag results in figure 6; that is, for $W_a = 0$, SCF = 1, and for large W_a, SCF $\propto \sqrt{(W_a/(1 + \alpha))}$.

Failing strains were predicted with equation (3) and compared with the test data. The values of K_Q, the elastic constants, and ε_{tu} used to make the calculations are given in reference 2 as "Manufacturer A" material.

Without stringers,

$$K_Q = S_{sh}\sqrt{\pi a + K_Q^2/F_{tu}^2} \qquad (1)$$

For uniaxial stress ($S_{sh} = E_{sh}\,\varepsilon_c$ and $F_{tu} = E_{sh}\,\varepsilon_{tu}$),

$$\frac{\varepsilon_{tu}}{\varepsilon_c} = \sqrt{1 + \frac{\pi a\,\varepsilon_{tu}^2 E_{sh}^2}{K_Q^2}} \qquad (2)$$

Where

$$SCF = \varepsilon_{tu}/\varepsilon_c$$

With stringers, replace a by $1/2\ W_a\ (Et)_{sh}/(Et)_1$

$$\frac{\varepsilon_{tu}}{\varepsilon_c} \sqrt{1 + \frac{\pi\, W_a\,(Et)_{sh}\,\varepsilon_{tu}^2 E_{sh}^2}{2\,(Et)_1\,K_Q^2}} \qquad (3)$$

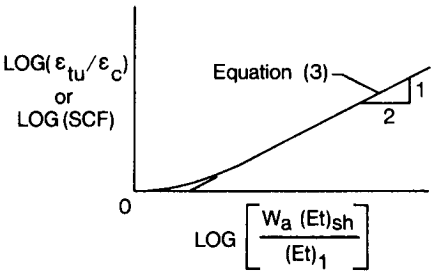

Figure 7

FAILING STRAIN VERSUS STRINGER THICKNESS

Failing strains are plotted against stringer thickness in figure 8 for panels in which cracks were arrested. Failing strains of panels without arrested cracks are not plotted. (As noted previously, they are usually larger than those of like panels with arrested cracks.) The panels had 1-inch-wide stringers and both $(45/0/-45/90)_{2s}$ and $(45/0/-45/0)_{2s}$ sheets. Predicted curves are plotted for comparison. For stringer thicknesses less than 20 or 30 plies, depending on sheet layup, the differences between measured and predicted failing strains are within the scatter among like specimens. For thicker stringers, equation (3) overestimates the failing strain. This discrepancy is probably due to out-of-plane effects, which give rise to strain gradients through the thickness. These strain gradients are not modeled in the plane analysis. They increase the membrane components of the crack tip strains by reducing the effective stiffness of the stringers, and they give rise to bending components. Both would reduce the failing strain of the panels.

Initially, three panels were made of each type. Some months later, an additional three panels of some types were made with stronger ends to avoid the possibility of failure in the grips. In some cases, both groups of the same type of panels failed in the test section, and the failing strains were noticeably different. (Data for panels that failed in the grips are not shown.) These discrepancies are usually apparent when there are more than three symbols, as for the 19-ply stringers in figure 8. Strain measurements indicate that the stiffnesses of the two groups of like panels are equal. Thus, the discrepancies are probably not due to an error in layup but may be due to differences in interface strength.

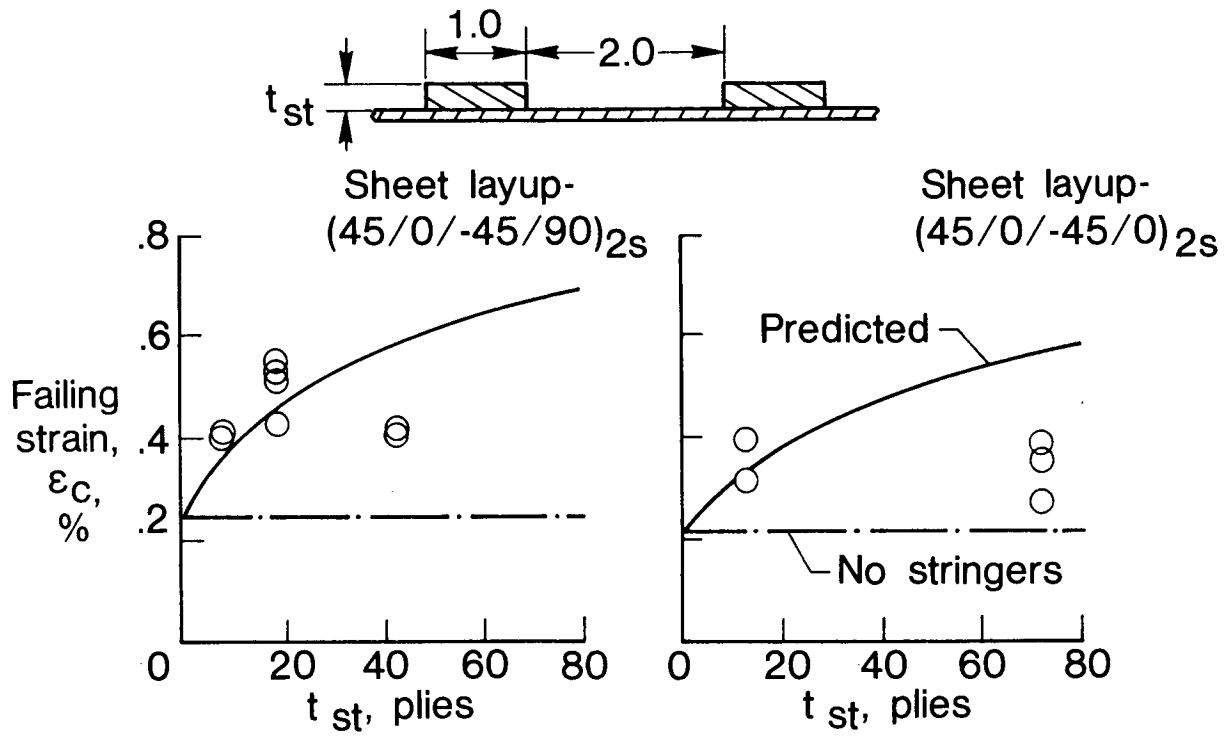

Figure 8

MODIFICATIONS TO ACCOUNT FOR OUT-OF-PLANE EFFECTS

To account for out-of-plane effects, $(Et)_1 = (Et)_{sh} + (Et)_{st}$ in equation (3) was replaced by $(Et)_1 = (Et)_{sh} + (Et)_{st}e^{-\gamma\alpha}$, where γ was determined to be 0.194 by fitting equation (3) to the data in figure 7 for panels with the thickest figure stringers of each sheet layup. The exponential factor was chosen because it is unity for small α and zero for large α. Predictions with the modified equation (3) are shown in figure 9 along with the results in figure 8. The original and the modified equation (3) give about the same results for the thinnest stringers. But, for thicker stringers, the modified equation agrees with the data and gives much lower failing strains.

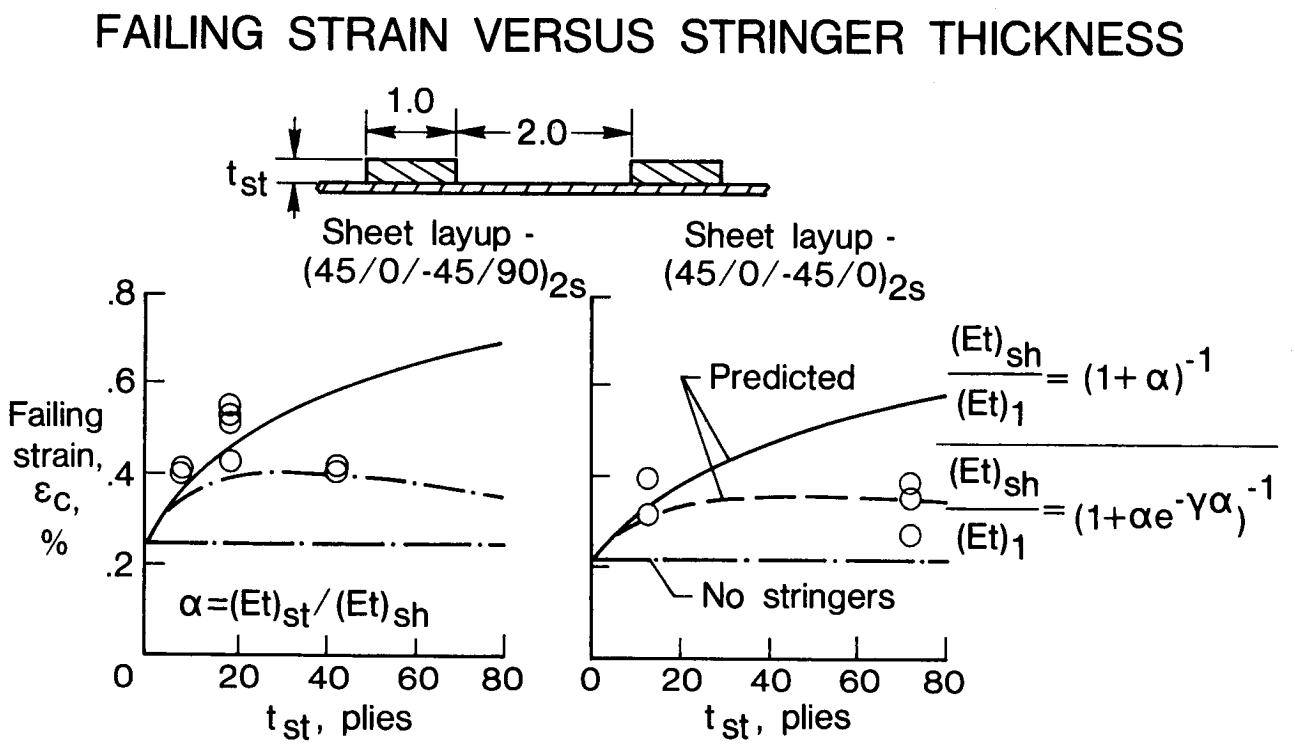

Figure 9

FAILING STRAIN VERSUS STRINGER SPACING

The failing strains are plotted against W_a in figure 10 for all the panels with a stringer stiffness ratio $\mu = 0.5$ and with arrested cracks. Values predicted with the modified equation (3) are also plotted for comparison. The measured and predicted failing strains agree. The differences are within the scatter among like specimens.

The results in figures 8 - 10 indicate that, due to the out-of-plane effects, an increase in stringer thickness above the 9 or 15 plies does not result in much further increase in failing strain.

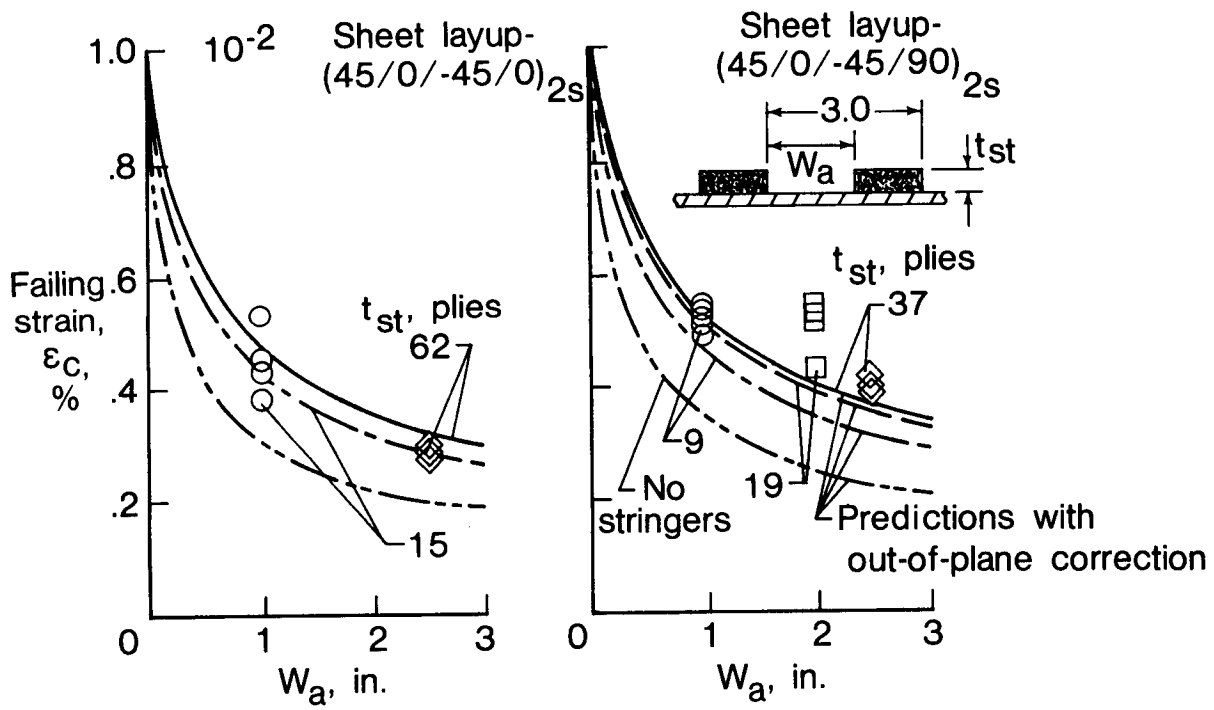

Figure 10

DESIGN CURVE FOR STIFFENED PANELS

It was shown in reference 3 that when crack tip damage is small, fracture toughness K_Q can be predicted with $K_Q = Q_c E_x/\xi$. The general fracture toughness parameter Q_c, in contrast to the fracture toughness K_Q, is independent of layup and varies only with ε_{tuf}, the fiber failing strain. For laminates with little or no crack tip damage, $Q_c = 0.30\ \varepsilon_{tuf}\sqrt{in.}$ The term $\xi = 1-\nu_{xy}\sqrt{(E_y/E_x)}$ accounts for the effect of sheet layup. The ν_{xy}, E_x, and E_y are the elastic constants of the sheet, where x denotes the loading direction.

Substituting the above equation for K_Q into equation (3) (modified to account for out-of-plane effects) and assuming that $\varepsilon_{tu} = \varepsilon_{tuf}$, a single design equation is produced for stiffened panels with any sheet layup and made of any material.

The resulting equation is shown as a single design curve in figure 11 by plotting the ratio of failing strains with and without cracks against $\xi^2 W_a/(1 + \alpha e^{-0.194\alpha})$. The $(45/0/-45/0)_{2S}$ data tend to be below the $(45/0/-45/90)_{2S}$ data because K_Q tends to be overpredicted for thin $(45/0/-45/0)_{2S}$ laminates and underpredicted for thin $(45/0/-45/90)_{2S}$ laminates (refs. 3 and 4). In comparison to scatter among like specimens, the agreement between the data and the design curve is good. A lower bound curve could be calculated using a value of $Q_c/\varepsilon_{tuf} < 0.30\ \sqrt{in.}$

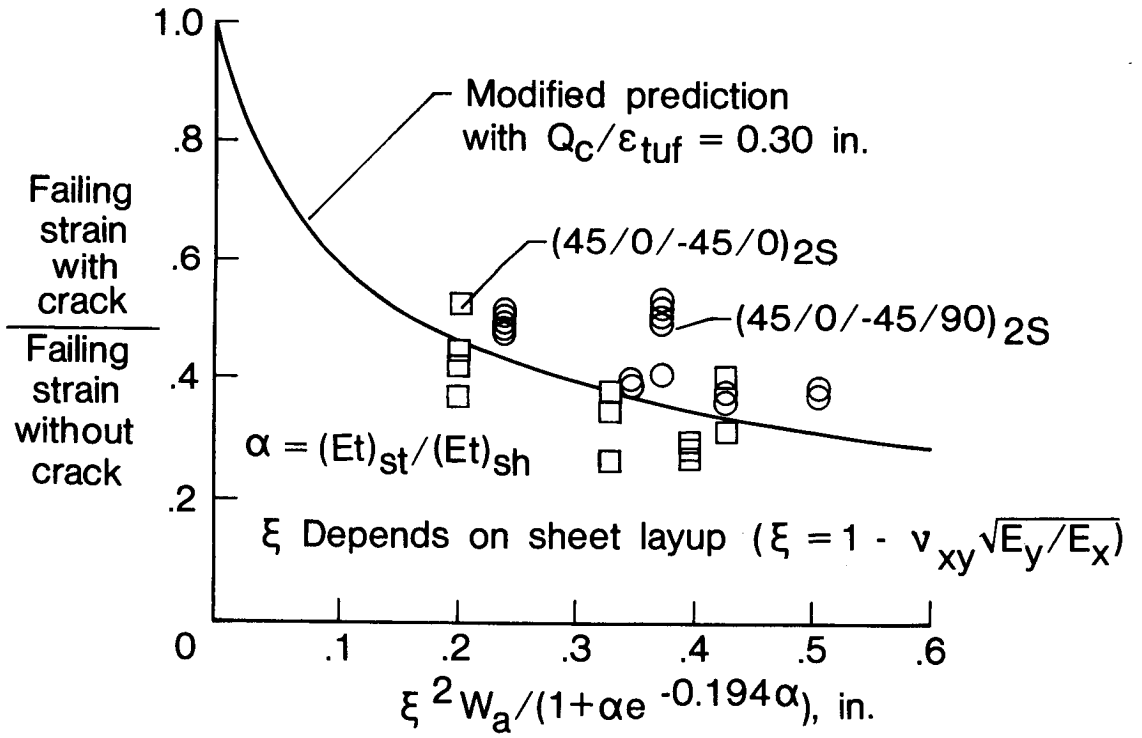

Figure 11

MAXIMUM PREDICTED IMPROVEMENT WITH STRINGERS

Equation (3) with $(Et)_{sh}/(Et)_1 = 1/(1 + \alpha e^{-0.194\alpha})$ predicts a maximum increase in failing strain of stiffened panels over unstiffened panels. Calculations of the ratio of failing strain with stringers to that without stringers is plotted against α in figure 12 for various values of W_a. The failing strain ratio has a maximum value at $\alpha = \alpha^*$, where $\alpha^* = 1/0.194$. The maximum value increases with W_a and asymptotically approaches 1.7. However, it is not very sensitive to W_a for $W_a > 1$ inch nor to α for $2 < \alpha < \alpha^*$. For the sheet layups here, $t_{st}/t_{sh} = 2.1$ and 2.9 for $\alpha = \alpha^*$. Note that the curve in figure 13 without the out-of-plane correction indicates no limit in improvement.

$$(Et)_{sh}/(Et)_1 = (1 + \alpha e^{-0.194\alpha})^{-1}$$

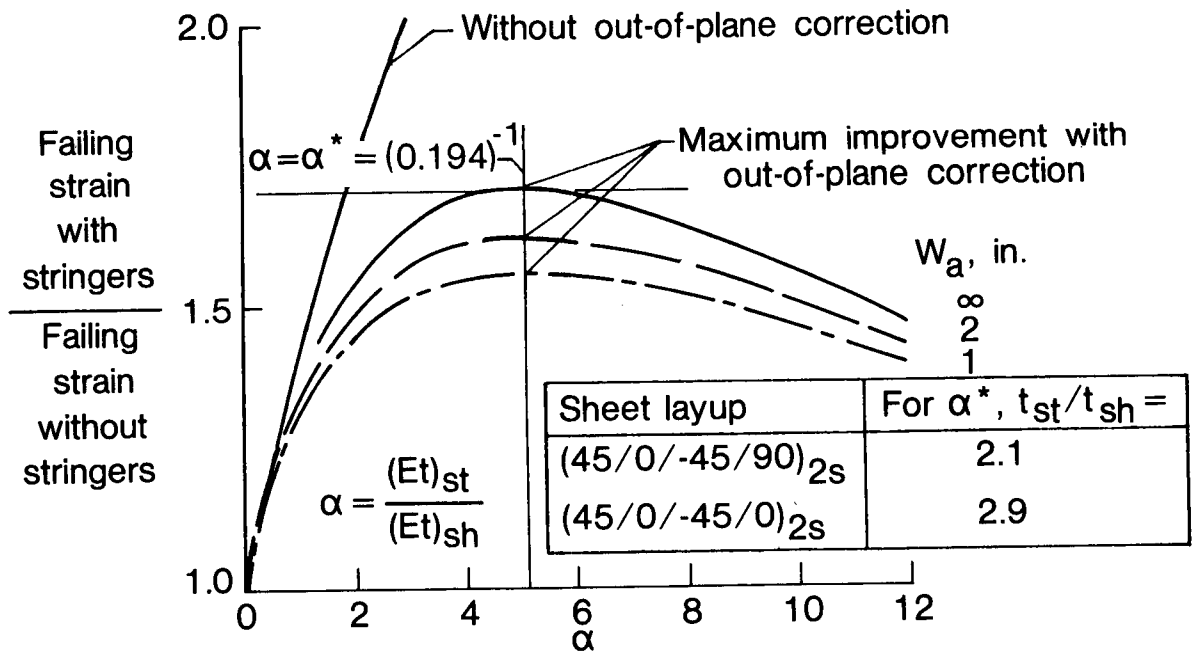

Sheet layup	For α^*, t_{st}/t_{sh} =
$(45/0/-45/90)_{2s}$	2.1
$(45/0/-45/0)_{2s}$	2.9

Figure 12

CONCLUSIONS

1. Bonded stringers can arrest cracks.

2. Stringers can increase failing strains as much as 80%.

3. Failing strains are larger for thicker and more closely spaced stringers.

4. Stringer width seems relatively unimportant.

5. Failing strains are a maximum when the thickness of unidirectional stringers is 2 to 3 times that of the sheet.

6. Very strong and stiff bonds or very weak bonds may weaken a sheet with bonded stringers.

7. A fracture mechanics analysis predicts the failing strains well.

8. A single design curve was developed using the analysis and the fracture toughness parameter Q_c.

REFERENCES

1. Arin, K.: "A Plate With a Crack, Stiffened By A Partially Debonded Stringer." Engineering Fracture Mechanics, 1974, Vol. 6, pp. 133-140.

2. Kennedy, J. M.: "Fracture Behavior of Hybrid Composite Laminates." AIAA/ASME/ASCE/AHS 24th Structures, Structural Dynamics and Materials Conference. Lake Tahoe, NV, May 2-4, 1983.

3. Poe, Jr., C. C.: "A Unifying Strain Criterion for Fracture of Fibrous Composite Laminates." Engineering Fracture Mechanics, Vol. 17, No. 2, pp. 153-171, 1983.

4. Harris, C. E.; and Morris, D. H.: "Fracture Behavior of Thick, Laminated Graphite/Epoxy Composites." NASA CR-3784, 1984.